This article has been accepted for publication in a future proceedings of this conference, but has not been fully edited. Content may change prior to final publication. Citation information: DOI10.1109/ICRA48891.2023.10160254, 2023 IEEE International Conference on Robotics and Automation (ICRA)

Author's accepted manuscript. Accepted 17-01-2023

Design and Development of a Novel Force-Sensing Robotic System for the Transseptal Puncture in Left Atrial Catheter Ablation

Aya Mutaz Zeidan[1], Zhouyang Xu[1], Christopher E. Mower[1], Honglei Wu[1], Quentin Walker[1], Oyinkansola Ayoade[1], Natalia Cotic[1], Jonathan Behar[1], Steven Williams[1], Aruna Arujuna[1], Yohan Noh[2], Richard Housden[1], and Kawal Rhode[1]

***Abstract*— Transseptal puncture (TSP) is a prerequisite for left atrial catheter ablation for atrial fibrillation, requiring access from the right side of the heart. It is a demanding procedural step associated with complications, including inadvertent puncturing and application of large forces on the tissue wall. Robotic systems have shown great potential to overcome such challenges by introducing force-sensing capabilities and increased precision and localization accuracy. Therefore, this work introduces the design and development of a novel robotic system developed to perform TSP. We integrated optoelectronic sensors into the tools' fixtures, measuring tissue contact and puncture forces along one axis. The novelty of this design is in the system's ability to manipulate a Brockenbrough (BRK) needle and dilator-sheath simultaneously and measure tissue contact and puncture forces. In performing puncture experiments on anthropomorphic tissue models, an average puncture force of 3.97 ± 0.45 N (1SD) was established - similar to the force reported in literature on the manual procedure. This research highlights the potential for improving patient safety by enforcing force constraints, paving the way to more automated and safer TSP.**

I. INTRODUCTION

Transseptal puncture (TSP) is necessary for left-sided atrial ablation for atrial fibrillation, enabling the passage of the ablation catheter from the right atrium to the left. It involves puncturing a small region within the interatrial septum (IAS) known as the fossa ovalis [1]. TSP is a technically demanding procedural step in left atrial ablation, with challenges brought about by complex anatomical atrial septum abnormalities, particularly during repeat transseptal catheterization [2]. It is associated with a steep learning curve - even for skilled operators - with a 1-2% incidence rate of major complications [3], in addition to a 2-3% incidence of cardiac perforation, pericardial effusion or tamponade, aortic root puncture, and atrial wall puncture for less skilled operators [4].

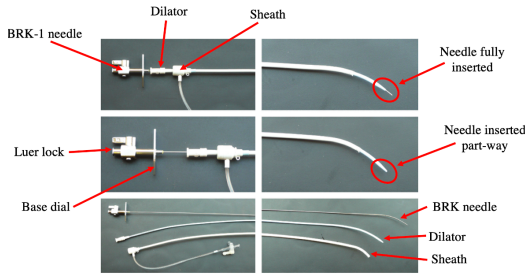

Fig. 1: Components of transseptal assembly: BRK needle (71cm), dilator (67cm), and transseptal sheath (63cm). Top image shows needle fully advanced into dilator to puncture fossa ovalis. Middle image shows needle part-way advanced into the needle [1].

The TSP kit (shown in Fig. 1), employed in this work, consisted of a standard 8.5 French transseptal sheath (SL0, St Jude Medical Inc. St Paul, MN, USA), a stiff dilator (Torflex Superstrong, Baylis Medical company, Inc. Montreal, Canada), and a BRK-1 (St Jude Medical Inc., St Paul, MN, USA). The adult BRK-1 needle has a 53° curved distal end to allow controlled rotation of the tip. The dilator-sheath (curvature 270°) is required to localize and deliver the BRK needle to the fossa ovalis [5].

There have been three commercial robotic catheter ablation systems: Niobe® Remote Magnetic Navigation (RMN) System (Stereotaxis Inc., St Louis, MO) [6]; Sensei® Robotic Navigation System (Hansen Medical, Inc., Mountain View, CA) [7]; and AMIGO^{TM} Remote Catheter System (Catheter Precision, Inc., Mount Olive, NJ, USA) [8]. Many ablation catheters include force sensing, such as the ThermoCool® SmartTouch® Catheter (Biosense Webster Inc., CA, USA) which provides real-time contact force data to exert force control during ablation [9]. Further, Saliba *et al.* designed an algorithm (IntelliSense, Hansen Medical) to constantly monitor the contact force exerted by the catheter tip to provide tactile feedback [10]. Exceeding the preset limit for the contact force would raise a visual alarm, preventing catheter advancement. Despite the success and

[1]A. M. Zeidan, Z. Xu, C. E. Mower, H. Wu, Q. Walker, O. Ayoade, N. Cotic, J. Behar, S. Williams, A. Arujuna, R. Housden, and K. Rhode are with the Department of Surgical & Interventional Engineering, School of Biomedical Engineering & Imaging Sciences, King's College London, London SE1 7EH, U.K. Email corresponding author: aya.zeidan@kcl.ac.uk.

[2]Y. Noh is with the Department of Mechanical and Aerospace Engineering, Brunel University London, Uxbridge UB8 3PH, U.K.

This research was supported by the Wellcome Centre for Medical Engineering at King's College London and the British Heart Foundation (BHF) Centre of Excellence at King's College London. The authors acknowledge support from the Department of Health and Social Care (DHSC) through the National Institute for Health and Care Research (NIHR) MedTech and Vitro Diagnostic Co-operative (MIC) award for Cardiovascular Diseases to Guy's St Thomas' NHS Foundation Trust in partnership with King's College London. Christopher E. Mower is supported by the FAROS project and has received funding from the European Union's Horizon 2020 research and innovation programme under grant agreement No 101016985.

This article has been accepted for publication in a future proceedings of this conference, but has not been fully edited. Content may change prior to publication. Citation information: DOI10.1109/ICRA48891.2023.10160254, 2023 IEEE International Conference on Robotics and Automation (ICRA)

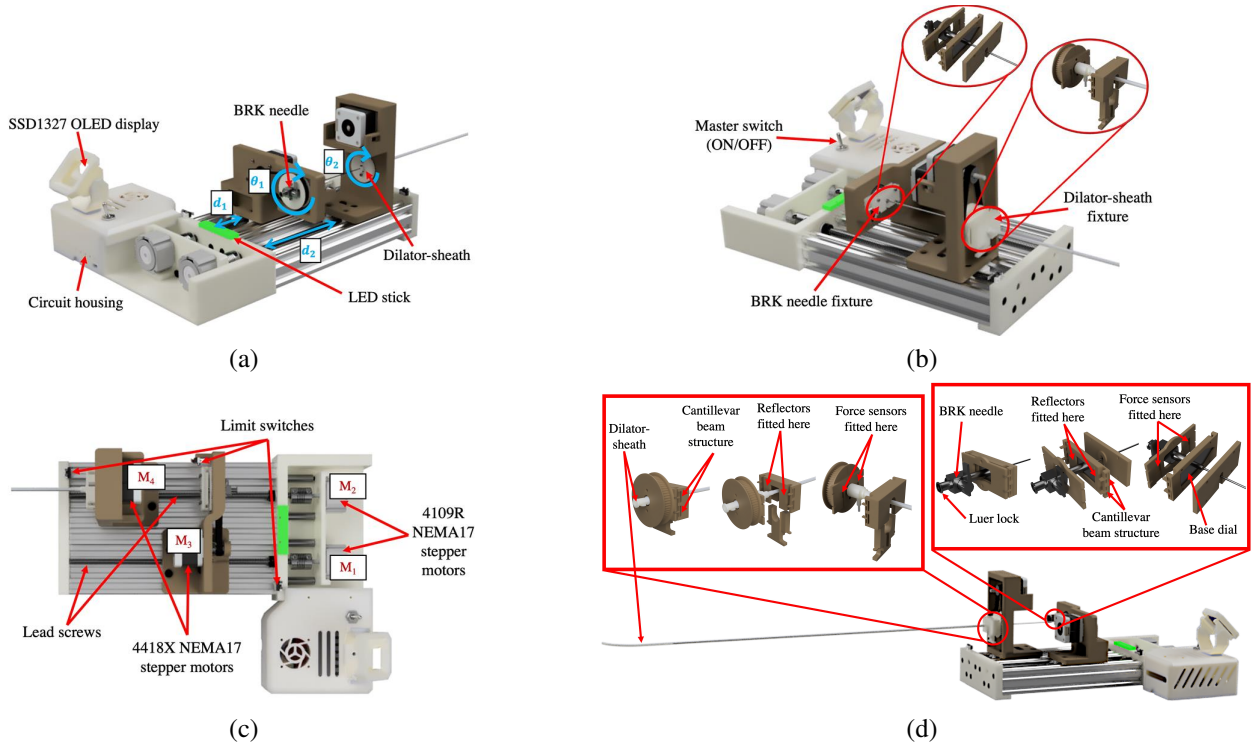

Fig. 2: Components of the robotic system designed in CAD software.

commercialization of these solutions, they do not consider TSP.

Sharma *et al.* provide a comprehensive review of devices and techniques for TSP [5]. Yet, they all require significant alteration of the conventional TSP kit (Figure 1). One example is the "all-in-one" integrated transseptal crossing device for TSP developed by Rizzi *et al.* [11]. Other examples include a radiofrequency needle for TSP [12], and a transseptal approach using a non-fluoroscopic technique [13], [14]. However, modification of the TSP kit would increase cost, making it less a feasible solution given its single-use functionality.

Minimally invasive surgery (MIS) enjoys several key benefits for the patient (e.g. reduced trauma, hospital stay, and recovery time). However, it impedes the cardiologist's ability to accurately monitor the interventional tools position and regulate the applied force at the tip. Furthermore, equipping sensors on the distal end of the tools is challenging due to their small size. Several teams have proposed a magnetic force sensor for MIS that aims to reduce the device's size while improving its robustness [15], [16], [17], [18]. For example, Chatzipirpiridis *et al.* combined a magnetic Hall sensor, a miniature permanent magnet and a thin film based on the principle of magnetic induction [15]. Although small, this sensor is complex to manufacture and has a relatively small measurement range. Other sensors include capacitive force sensors and optical sensors. In [19] and [20], capacitive array haptic sensors were used to collect information on organ palpation, including changes in shape and stiffness, due to their high sensitivity. Several teams have demonstrated the use of fiber optic sensors for catheter force measurement in MIS [21], [22], [23], [24]. Optical force sensing is a powerful choice due to its small size and precision. The most commonly used technique in the application of fiber optic sensing is optical intensity modulation, where its advantages were demonstrated in the development of triaxial force sensors in [23]. However, this approach is associated with a high monetary cost.

In order to reduce the possibility of complications, online and accurate readings of the contact forces between the needle tip and IAS are essential [25], [26], [27], [28], [29]. The integration of force feedback into the TSP kit offers excellent opportunities to improve puncture safety.

A robotic TSP system with force-sensing capabilities can be an effective tool in ablation procedures due to its potential to achieve more dexterous, precise, and accurate tool manipulation compared to the manual procedure [30]. This conclusion can also be generalized from the clinical trials conducted on commercial catheter ablation robotic systems [6], [31], [32], [33], [34]. This work is motivated by a lack of robotic systems developed for addressing the TSP procedural step in left atrial cardiac ablation.

Our research makes the following contributions:

1) ***Novel robot*** system design that incorporates ***force-sensing capabilities*** for measuring uniaxial contact and puncture forces on the distal ends of the BRK needle and dilator-sheath. This is the first of its kind.
2) ***Cooperation of tools:*** Our prototype was designed to achieve cooperation of the BRK needle and dilator-sheath, permitting their simultaneous manipulation.

This article has been accepted for publication in a future proceedings of this conference, but has not been fully edited. Content may change prior to publication. Citation information: DOI10.1109/ICRA48891.2023.10160254, 2023 IEEE International Conference on Robotics and Automation (ICRA)

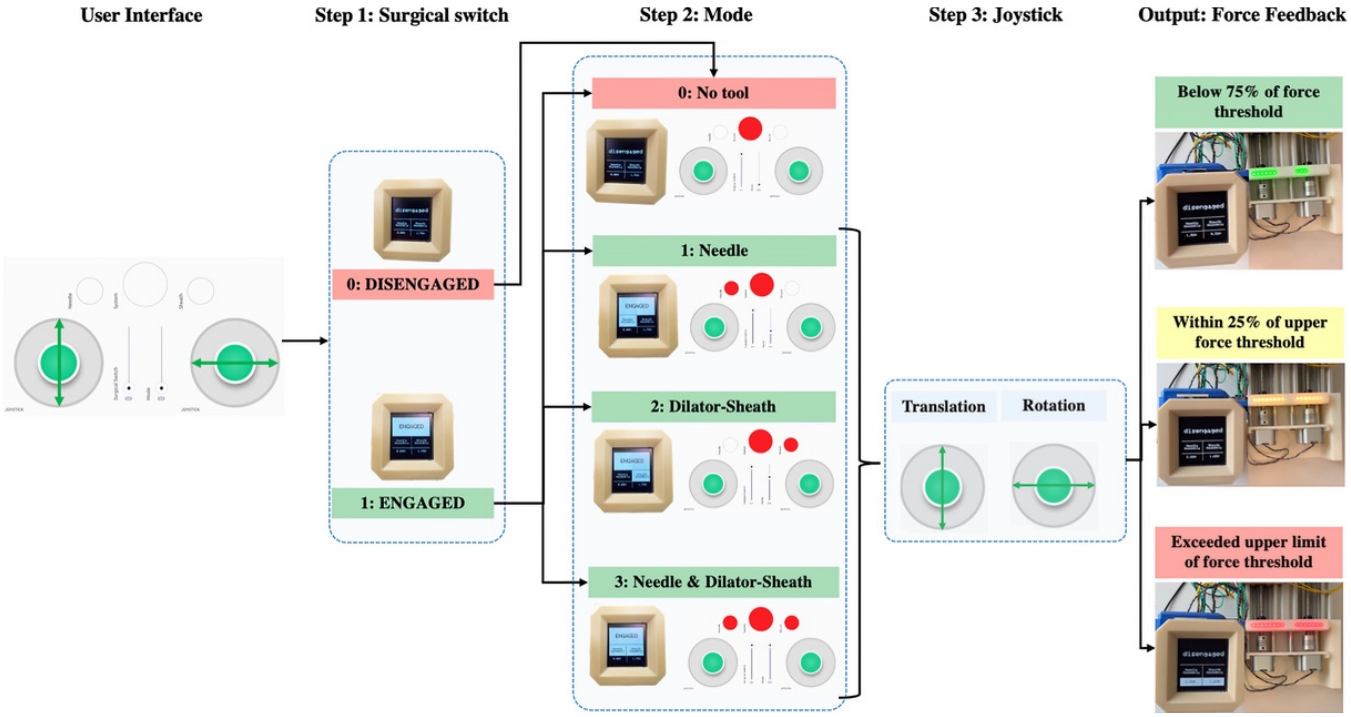

Fig. 3: User interface on Blynk application used to define the desired task-space position of the tool tip. The green circles represent the joysticks. The left slider turns the surgical switch on and off. The right slider permits selection of tool mode (highlighted in red circles at the top of the interface).

Coordinated control of the tools in the TSP kit is required to navigate to a desired location on the IAS.

3) ***Use of conventional TSP kit:*** The TSP kit is operated accurately and in a stable manner (as the kit is firmly secured to the system). Further, the goal was not to modify the TSP kit, but rather to assist the cardiologist in performing the procedure using the conventional TSP kit by equipping them with additional capabilities. The TSP kit is single-use, therefore it was essential to ensure that the system's modular design would ease replacement of the needle and dilator-sheath between ablation procedures.

There is no robotic system available that can fulfill all three requirements to the best of our knowledge. Our research addresses these challenges using a novel TSP robotic system.

II. Design Methods and Fabrication

The purpose of this section is to describe the design and development of our novel TSP system, the user interface for remote control, safety features integrated into the system design, and the incorporation of force-sensing capabilities to measure tissue contact and puncture forces.

A. Model Description

The cardiologist controls the BRK needle and dilator-sheath from outside the body, pivoting it about the puncture site on the femoral vein [1]. This restricts the number of degrees of freedom (DoFs) of the procedure to 2 DoFs. Rotation is required to rotate the curved needle tip and dilator-sheath to locate the fossa ovalis. Cardiologists manipulate the tools via a cooperation principle of the BRK needle and dilator-sheath using the following motions: (1) independent rotation and translation of the needle; (2) independent rotation and translation of the dilator-sheath; and (3) combined rotation and translation of the needle and dilator-sheath.

The TSP system (refer to Fig. 2) comprises of a fixed base frame and four movable joints. Four independent stepper motors, identified as M_{1-4}, were employed for independent rotation and translation of the BRK needle and dilator-sheath. The BRK needle and dilator-sheath are attached to the manipulator by mounting them into the fixtures illustrated in Fig. 2d. Motors M_1 and M_2 are 4109R NEMA-17 bipolar stepper motors (0.9° step angle, 400 steps/revolution) (Lin Engineering Inc., Morgan Hill, CA, USA) and M_3 and M_4 are 4418X NEMA-17 bipolar motors (1.8° step angle, 200 steps/revolution) (Lin Engineering Inc., Morgan Hill, CA, USA). Lead screws are attached to motors M_1 and M_2 for linear translation of the BRK needle and dilator-sheath, while M_3 and M_4 are used for continuous rotation of the needle and sheath. Thus, this system implements 4 DoFs. When the needle and dilator-sheath are fully coupled – i.e., the needle is fully inserted in the dilator-sheath – the system is able to achieve a maximum driving length of 144.5 mm.

The fixture housing the needle (seen in Fig. 2d) was designed to provide the cardiologist with access to the Luer

This article has been accepted for publication in a future proceedings of this conference, but has not been fully edited. Content may change prior to publication. Citation information: DOI10.1109/ICRA48891.2023.10160254, 2023 IEEE International Conference on Robotics and Automation (ICRA)

lock during the procedure - essential to flush the needle. The same principle was applied for the fixture housing the dilator-sheath, where the top of the dilator was free from obstruction to provide the needle with an entry point into the dilator-sheath. During TSP, a force would be applied on the distal ends of the needle and sheath. In this work, the force is measured on the proximal end (where a cardiologist would manipulate the tools during the manual procedure).

Computer-aided design (Fusion 360, Autodesk, USA), additive manufacturing of fused deposition modeling (FDM) (Prusa, Prusa Research, Czech Republic), and stereolithography (SLA) (Form 3+, Formlabs, Somerville, MA, USA) were employed in the manufacturing process.

B. Remote Control and User Interface

We implemented an open control loop that tracks a desired task-space position. The needle and dilator-sheath tips each have 2 DoFs in the task space, and 4 actuation DoFs to ensure that the needle and dilator-sheath tips reach the anatomical target. To achieve this, an interface was developed using internet of things (IoT) Blynk application as the input modality for remote control, permitting the user to remotely operate the system with an iOS or Android mobile. The purpose of this was to evaluate the performance of the system in performing TSP rather than the latency.

An Arduino MKR WIFI 1010 (Arduino LLC, Italy) was used in this work and connected to the internet via a WiFi access point. The response latency was 30 ms. The operating modes, illustrated in Fig. 3, are controlled in the following order:

- ***Step 1 - Surgical switch:*** The first step is to enable the joystick interface by "engaging" the system. When system is "disengaged", all four stepper motors are disabled.
- ***Step 2 - Mode:*** By engaging the system, the operator has three modes to select from: (1) independent control of the needle module; (2) independent control of the dilator-sheath module; (3) simultaneous control of the needle and dilator-sheath modules.
- ***Step 3 - Joystick:*** The left joystick permits translational motion (M_1 and M_2), while the right joystick permits rotational motion (M_3 and M_4).
- ***Output - Force information:*** The LED offers a visual indication of the force experienced by each module, while the OLED displays the values for force exerted by the TSP kit.

C. Safety Features

We implemented the following safety features:

- **Toggle switch** was used as the master switch to turn off all the components, preventing the system from being inadvertently driven.
- Three **limit switches** were used to enforce hard constraints on the position, preventing: (1) needle gantry from colliding with the back end of the base frame; (2) dilator-sheath gantry from colliding with the front end of the base frame; (3) needle and dilator-sheath gantries from colliding with one another when needle is driven into the sheath to be fully inserted during puncture.
- The **LED strip** was used as a visual indicator of the force measured on the tips of the needle and dilator-sheath, as well as indicate how much the force was within a preset threshold: green indicated that the applied contact force below 75% of the force threshold and provides the cardiologist with a real-time reading of the force applied; yellow was used to warn the cardiologist that the force was within 25% of the upper threshold; and red was used as a visual alarm to indicate that the applied force had exceeded the preset limit, resulting in a hard motion constraints being applied on the entire system, which is the point at which the the motion of the needle and/or dilator-sheath was limited in the direction that the force was being applied. This would prevent the distal end of the tools from exerting excessive forces on the patient.
- The **OLED display** highlighted which tool was being driven and the values for the force applied on the tissue by the needle and dilator-sheath. It also indicated whether the surgical switch was on or not, and the tool that was being driven at each point in time.

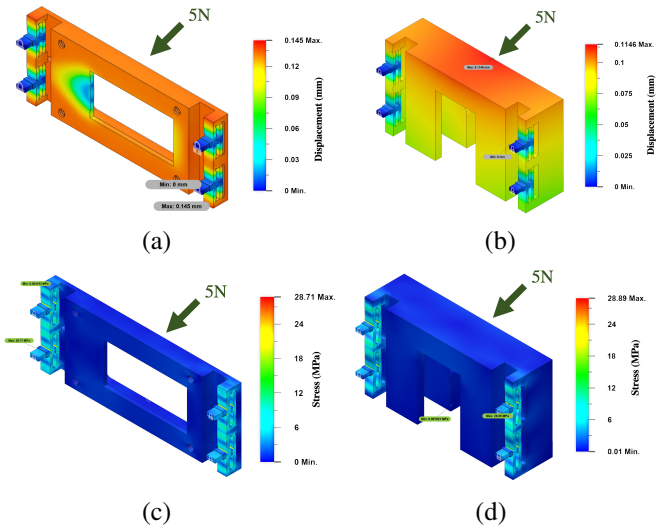

Fig. 4: FEM simulation of stress, performed in Fusion360, applying a force, F_z, of 5 N on the (a) needle and (b) dilator-sheath fixtures. The corresponding Von Mises stress for the (c) needle and (d) dilator-sheath fixtures.

D. Integrating Force-Sensing in Fixture Designs

To measure the needle puncture force and the tissue contact force applied from the dilator-sheath along the long-axis (uniaxial), optoelectronic sensors were integrated into the needle and dilator-sheath fixtures. The optoelectronic sensor chosen for this research was the NJL5901R-2 (New Japan Radio Co., Ltd, Japan) - a low-cost, miniaturized, compact surface mount type photo reflector (1.0 x 1.4 x 0.6 mm). The basic structure of the optoelectronic sensor

This article has been accepted for publication in a future proceedings of this conference, but has not been fully edited. Content may change prior to publication. Citation information: DOI10.1109/ICRA48891.2023.10160254, 2023 IEEE International Conference on Robotics and Automation (ICRA)

is based on four components: a light-emitting diode (LED), a phototransistor, a cantilever beam structure, and a reflector.

The cantilever structure utilizes the basic principle of intensity modulation of light. Applying an external force on the cantilever beam resulted in the deformation shown in Fig. 4. The difference in the reflected light was given by a variable voltage output from the sensor. Mounted on each fixture were two NJL5901R-2 optoelectronic sensors on either side of the tools. This resulted in two output voltage readings, which were then averaged to obtain a single voltage value and converted to force using quadratic least square regression. A similar design was applied to both the needle and dilator-sheath fixtures for uniformity across the system. The fixture was developed using Tough 2000 Resin - the most resilient material of Engineering Resins [35]. This ensured flexibility of the cantilever structure and its ability to recover after deforming.

III. Tests and Performance

In this section we describe the development an anthropomorphic fossa ovalis tissue model for the purpose of testing the tissue contact and puncture forces measured by the force sensors. This was then followed by deformation testing of the fixture structures, as well as puncture force experiments to evaluate the system's force-sensing capabilities.

A. Fossa Ovalis Tissue Model

A two-part injection mold of the fossa ovalis was printed in Clear Resin (Formlabs Photopolymer Clear Resin). The mold was designed with a variable thickness of 2.5 mm on the edge and 1.8 mm in the center. A two-part silicone mixture of 00-50 and thinner were mixed together to create a 00-35 silicone rubber. After filling the mold with the mixture, it was rested in a vacuum chamber (Fisherbrand, Fisher Scientific, Loughborough, UK) under 800 mmHg vacuum pressure to degas the air bubbles. The silicone was then allowed to cure for 3 hours before being removed from the mold.

B. Deformation Testing of Fixture Structures

Finite element method (FEM) simulation was conducted to assess the degree of deformation of the cantilever beam structure. The material property values in this simulation were set at: yield strength of 41 N/m^2, mass density of 1.172E-06 kg/mm^3, Young's modulus of 2.21 GPa; these assumptions were based on information provided by Formlabs. As shown in Figs. 4a and 4b, the cantilever structures in both fixtures underwent a deformation of 0.1 mm, while a negligible deformation (<0.05 mm) was experienced by the other portions of the fixture. This value is within the optimal range for the reflector distance (measuring distances <0.2 mm) for the NJL5901R-2 sensor to produce the maximum relative output current of 100%. The maximum Von Mises stress observed in Figs. 4c and 4d was found to be under 30 MPa, which is well below the ultimate tensile strength of Tough 2000 Resin at 49 MPa.

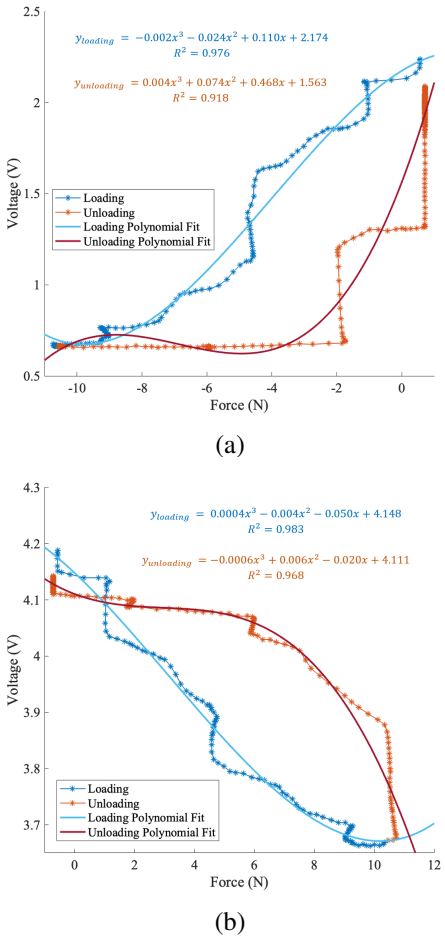

Fig. 5: Calibration of NJL5901R-2 voltage: characteristic curves of output voltage and force of the sensors in (a) needle and (b) sheath fixtures.

C. Puncture Testing

The output voltage from the NJL5901R-2 sensors was calibrated with force measured with an ATI Nano17 force transducer (ATI Industrial Automation, Apex, NC, USA), outputting the characteristic curves in Figs. 5a and 5b. A third-order polynomial was used to model the relationship between the desired force and required voltage.

Ten punctures were performed on individual fossa ovalis tissue models, where the required puncture force was recorded, as well as the forces required to pass various portions of the TSP kit through the tissue model. The experimental setup in Fig. 6 consisted of an aluminum profile on which a tube (mimicking the vein in which the TSP kit would pass through in the manual procedure) was fixed on to guide the TSP kit to the fossa ovalis tissue model at the end of the profile, to perform TSP.

Using the system to perform TSP, a puncture force of 3.97 ± 0.45 N (1SD) was established, which is greater than that measured by [25] of 1.97 ± 0.74 N. The dilator puncture force in our work was found to be 3.57 ± 0.50 N (1SD).

This article has been accepted for publication in a future proceedings of this conference, but has not been fully edited. Content may change prior to publication. Citation information: DOI10.1109/ICRA48891.2023.10160254, 2023 IEEE International Conference on Robotics and Automation (ICRA)

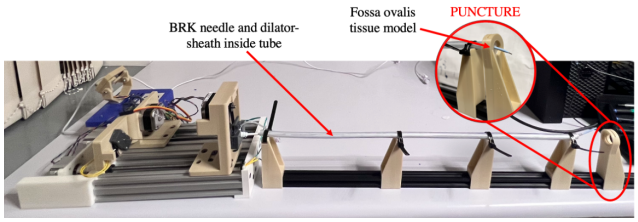

Fig. 6: Experiment setup for force testing consisting of a tube acting as the femoral vein, guiding the TSP kit to the fossa ovalis at the right end of the setup.

The increased force exerted by the tapered portion of the dilator, as it passed through the puncture site, was required to expand the fossa ovalis [25].

Distinctive peaks during each transition of the needle and dilator-sheath can be noted in Fig. 7. The average maximum puncture force applied by the BRK needle was 3.97 N, while the average maximum force of the dilator puncture was measured to be 3.57 N.

IV. Discussion

In the present work, a novel robotic TSP system was proposed to manipulate the conventional TSP kit. The key novelty is in its ability to be operated to manipulate the tools independently or simultaneously, while providing the cardiologists with: (1) easy access to the TSP kit to flush the tools during the procedure; (2) the ability to dispense the tools and replace them in between procedures; (3) information on contact and puncture forces; and (4) safe tool manipulation due to integrated safety features.

Our system could potentially reduce radiation exposure for patients and physicians. This conclusion is derived from the efficacy of catheter robotic systems in reducing fluoroscopy time, as validated in clinical studies [36], [37], [38], [39]. Moreover, it can provide increased precision of tool localization, resulting in increased dexterity of the catheter passing through the puncture site [30].

The system can additionally be employed for pre-surgical planning with cardiac phantoms, or used to aid trainees in learning the steps to perform the procedure rather than the skills required to manually perform the procedure. This would reduce the steep learning curve of the procedure for trainees or less skilled operators [40].

Another crucial advantage of our system is that there is no modification of the conventional TSP kit, thus decreasing its cost and ensuring its feasibility. It further progresses the state-of-the-art by improving the safety of the intervention through the use of the safety features described in Section II-C and force information, which would decrease the risk of complications such as cardiac perforation and tamponade.

From experimental testing, we concluded that such a system can improve safe interactions between the TSP kit and the IAS. Despite the difference in puncture force observed between our results and that from [25], the force applied by the TSP system was not significantly greater than that of the manual procedure. Yet, the orientation of the fossa ovalis was a limitation affecting the validity of the results. Objective experiments are necessary to validate the tissue properties of the fossa ovalis model developed in this work, and ensure it did not introduce bias during force testing.

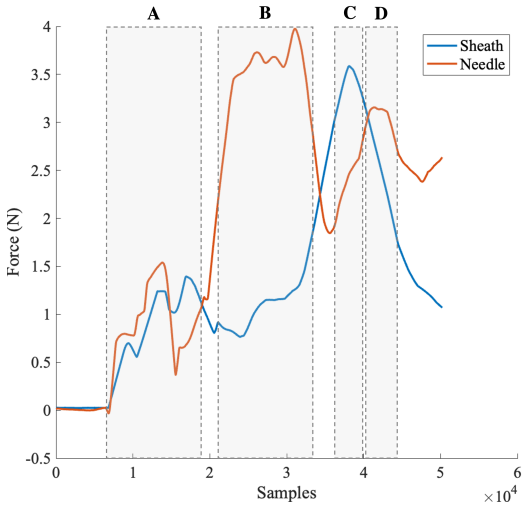

Fig. 7: Force over time during fossa ovalis puncturing, taken as an average of 10 punctures, performed on fossa ovalis tissue models. The peaks are labeled as follows: **A**, contact force applied by needle and dilator-sheath during fossa ovalis localization; **B**, needle puncture; **C**, dilator puncture; **D**, needle retracting from fossa ovalis.

The NJL5901R-2 offers a more miniaturized sensing configuration compared to the industrial standard ATI Nano17. It was also an ideal selection for sensor due to its rise response time of 20 μs and fall response time of 20 μs (as given in the datasheet). However, the hysteresis (one-axis) and creep phenomena in Fig. 5 occur to a considerable extent, signifying the slow recovery of the material after the physical load is removed. The use of Tough 2000 Resin for the structure of the cantilever beam may be the source of this delay in unloading, and thus must be addressed in future research to improve the accuracy of the force measurements.

V. Conclusion and Future Work

This paper presented a novel design for a robotic TSP system. We integrated force-sensing capabilities to prevent exertion of excessive contact and puncture forces on the patient. It was demonstrated that the embedded sensors were able to measure forces during TSP.

We evaluated the method by performing experiments on an anthropomorphic fossa ovalis tissue model to establish values for force applied during TSP using our system, and comparing it to literature values. Further, we developed an interface for online remote control of the TSP system, combining it with force-sensing to enforce hard motion constraints. These indicate the potential of the method to assist cardiologists in TSP.

Our future work will investigate the manual and automated control of the robotic system for performing TSP, and evaluate the tool tracking capabilities of the system.

This article has been accepted for publication in a future proceedings of this conference, but has not been fully edited. Content may change prior to publication. Citation information: DOI10.1109/ICRA48891.2023.10160254, 2023 IEEE International Conference on Robotics and Automation (ICRA)

REFERENCES

[1] M. J. Earley, "How to perform a transseptal puncture," *Heart*, vol. 95, no. 1, pp. 85–92, 2009.

[2] M. Almendárez, R. Alvarez-Velasco, I. Pascual, A. Alperi, C. Moris, and P. Avanzas, "Transseptal puncture: Review of anatomy, techniques, complications and challenges, a critical view," *International Journal of Cardiology*, 2022.

[3] N. Naik, "How to perform transeptal puncture," *Indian heart journal*, vol. 67, no. 1, p. 70, 2015.

[4] M. Alkhouli, C. S. Rihal, and D. R. Holmes, "Transseptal techniques for emerging structural heart interventions," *JACC: Cardiovascular Interventions*, vol. 9, no. 24, pp. 2465–2480, 2016.

[5] S. P. Sharma, R. Nalamasu, R. Gopinathannair, C. Vasamreddy, and D. Lakkireddy, "Transseptal puncture: devices, techniques, and considerations for specific interventions," *Current Cardiology Reports*, vol. 21, no. 6, pp. 1–7, 2019.

[6] M. N. Faddis, J. Chen, J. Osborn, M. Talcott, M. E. Cain, and B. D. Lindsay, "Magnetic guidance system for cardiac electrophysiology: a prospective trial of safety and efficacy in humans," *Journal of the American College of Cardiology*, vol. 42, no. 11, pp. 1952–1958, 2003.

[7] V. Y. Reddy, P. Neuzil, Z. J. Malchano, R. Vijaykumar, R. Cury, S. Abbara, J. Weichet, C. D. McPherson, and J. N. Ruskin, "View-synchronized robotic image-guided therapy for atrial fibrillation ablation: experimental validation and clinical feasibility," *Circulation*, vol. 115, no. 21, pp. 2705–2714, 2007.

[8] E. M. Khan, W. Frumkin, G. A. Ng, S. Neelagaru, F. M. Abi-Samra, J. Lee, M. Giudici, D. Gohn, R. A. Winkle, J. Sussman *et al.*, "First experience with a novel robotic remote catheter system: Amigo™ mapping trial," *Journal of Interventional Cardiac Electrophysiology*, vol. 37, no. 2, pp. 121–129, 2013.

[9] W. Ullah, A. McLean, M. H. Tayebjee, D. Gupta, M. R. Ginks, G. A. Haywood, M. O'Neill, P. D. Lambiase, M. J. Earley, R. J. Schilling *et al.*, "Randomized trial comparing pulmonary vein isolation using the smarttouch catheter with or without real-time contact force data," *Heart Rhythm*, vol. 13, no. 9, pp. 1761–1767, 2016.

[10] W. Saliba, J. E. Cummings, S. Oh, Y. Zhang, T. N. Mazgalev, R. A. Schweikert, J. D. Burkhardt, and A. Natale, "Novel robotic catheter remote control system: feasibility and safety of transseptal puncture and endocardial catheter navigation," *Journal of cardiovascular electrophysiology*, vol. 17, no. 10, pp. 1102–1105, 2006.

[11] S. Rizzi, L. Pannone, C. Monaco, A. Bisignani, V. Miraglia, A. Gauthey, G. Bala, M. Al Housari, F. Lipartiti, J. Mojica *et al.*, "First experience with a transseptal puncture using a novel transseptal crossing device with integrated dilator and needle," *Journal of Interventional Cardiac Electrophysiology*, pp. 1–7, 2022.

[12] M. Tokuda, S. Yamashita, S. Matsuo, M. Kato, H. Sato, H. Oseto, E. Okajima, H. Ikewaki, R. Isogai, K. Tokutake *et al.*, "Radiofrequency needle for transseptal puncture is associated with lower incidence of thromboembolism during catheter ablation of atrial fibrillation: propensity score-matched analysis," *Heart and Vessels*, vol. 33, no. 10, pp. 1238–1244, 2018.

[13] M. Mansour, M. R. Afzal, S. Gunda, J. Pillarisetti, K. Heist, M. R. Acha, M. Heard, J. Ruskin, and D. Lakkireddy, "Feasibility of transseptal puncture using a nonfluoroscopic catheter tracking system," *Pacing and Clinical Electrophysiology*, vol. 38, no. 7, pp. 791–796, 2015.

[14] G. Ballesteros, P. Ramos Ardanaz, R. Neglia, M. Palacio Solis, C. Diaz Fernandez, G. Lopez Gonzalez, E. Janiashvili, and I. GARCÍA-BOLAO, "Mediguide-assisted transseptal puncture without echocardiographic guidance," *Pacing and Clinical Electrophysiology*, vol. 40, no. 5, pp. 545–550, 2017.

[15] G. Chatzipirpiridis, P. Erne, O. Ergeneman, S. Pané, and B. J. Nelson, "A magnetic force sensor on a catheter tip for minimally invasive surgery," in *2015 37th Annual International Conference of the IEEE Engineering in Medicine and Biology Society (EMBC)*. IEEE, 2015, pp. 7970–7973.

[16] T. Le Signor, N. Dupré, and G. F. Close, "A gradiometric magnetic force sensor immune to stray magnetic fields for robotic hands and grippers," *IEEE Robotics and Automation Letters*, vol. 7, no. 2, pp. 3070–3076, 2022.

[17] H. Wang, G. De Boer, J. Kow, A. Alazmani, M. Ghajari, R. Hewson, and P. Culmer, "Design methodology for magnetic field-based soft tri-axis tactile sensors," *Sensors*, vol. 16, no. 9, p. 1356, 2016.

[18] T. P. Tomo, A. Schmitz, W. K. Wong, H. Kristanto, S. Somlor, J. Hwang, L. Jamone, and S. Sugano, "Covering a robot fingertip with uskin: A soft electronic skin with distributed 3-axis force sensitive elements for robot hands," *IEEE Robotics and Automation Letters*, vol. 3, no. 1, pp. 124–131, 2017.

[19] B. L. Gray and R. S. Fearing, "A surface micromachined microtactile sensor array," in *Proceedings of IEEE International Conference on Robotics and Automation*, vol. 1. IEEE, 1996, pp. 1–6.

[20] R. D. Howe, W. J. Peine, D. Kantarinis, and J. S. Son, "Remote palpation technology," *IEEE Engineering in Medicine and Biology Magazine*, vol. 14, no. 3, pp. 318–323, 1995.

[21] S. Hirose and K. Yoneda, "Development of optical six-axial force sensor and its signal calibration considering nonlinear interference," in *Proceedings., ieee international conference on robotics and automation*. IEEE, 1990, pp. 46–53.

[22] J. Peirs, J. Clijnen, D. Reynaerts, H. Van Brussel, P. Herijgers, B. Corteville, and S. Boone, "A micro optical force sensor for force feedback during minimally invasive robotic surgery," *Sensors and Actuators A: Physical*, vol. 115, no. 2-3, pp. 447–455, 2004.

[23] Y. Noh, S. Sareh, H. Würdemann, H. Liu, J. Back, J. Housden, K. Rhode, and K. Althoefer, "Three-axis fiber-optic body force sensor for flexible manipulators," *IEEE Sensors Journal*, vol. 16, no. 6, pp. 1641–1651, 2015.

[24] N. Bandari, J. Dargahi, and M. Packirisamy, "Miniaturized optical force sensor for minimally invasive surgery with learning-based nonlinear calibration," *IEEE Sensors Journal*, vol. 20, no. 7, pp. 3579–3592, 2019.

[25] S. A. Howard, S. G. Quallich, M. A. Benscoter, B. C. Holmgren, C. D. Rolfes, and P. A. Iaizzo, "Tissue properties of the fossa ovalis as they relate to transseptal punctures: a translational approach," *Journal of interventional cardiology*, vol. 28, no. 1, pp. 98–108, 2015.

[26] A. A. Elagha, A. H. Kim, O. Kocaturk, and R. J. Lederman, "Blunt atrial transseptal puncture using excimer laser in swine," *Catheterization and Cardiovascular Interventions*, vol. 70, no. 4, pp. 585–590, 2007.

[27] L. Capulzini, G. Paparella, A. Sorgente, C. De Asmundis, G. B. Chierchia, A. Sarkozy, A. Muller-Burri, Y. Yazaki, M. Roos, and P. Brugada, "Feasibility, safety, and outcome of a challenging transseptal puncture facilitated by radiofrequency energy delivery: a prospective single-centre study," *Europace*, vol. 12, no. 5, pp. 662–667, 2010.

[28] M. Wieczorek, R. Hoeltgen, E. Akin, and A. R. Salili, "Use of a novel needle wire in patients undergoing transseptal puncture associated with severe septal tenting," *Journal of interventional cardiac electrophysiology*, vol. 27, no. 1, pp. 9–13, 2010.

[29] M. J. McWILLIAMS and P. Tchou, "The use of a standard radiofrequency energy delivery system to facilitate transseptal puncture," *Journal of cardiovascular electrophysiology*, vol. 20, no. 2, pp. 238–240, 2009.

[30] J. Jayender, R. Patel, G. Michaud, and N. Hata, "Optimal transseptal puncture location for robot-assisted left atrial catheter ablation," *The International Journal of Medical Robotics and Computer Assisted Surgery*, vol. 7, no. 2, pp. 193–201, 2011.

[31] G. Bassil, S. M. Markowitz, C. F. Liu, G. Thomas, J. E. Ip, B. B. Lerman, and J. W. Cheung, "Robotics for catheter ablation of cardiac arrhythmias: Current technologies and practical approaches," *Journal of Cardiovascular Electrophysiology*, vol. 31, no. 3, pp. 739–752, 2020.

[32] A. Da Costa, M. B. H'Dech, C. Romeyer-Bouchard, L. Bisch, A. Gate-Martinet, M. Levallois, and K. Isaaz, "Remote-controlled magnetic pulmonary vein isolation using a new three-dimensional non-fluoroscopic navigation system: a single-centre prospective study," *Archives of cardiovascular diseases*, vol. 106, no. 8-9, pp. 423–432, 2013.

[33] A. Tolga, S. Bozyel, E. Golcuk, K. Yalin, and T. E. Guler, "Atrial fibrillation ablation using magnetic navigation comparison with conventional approach during long-term follow-up," *Journal of Atrial Fibrillation*, vol. 8, no. 3, 2015.

[34] A. Da Costa, J. B. Guichard, C. Roméyer-Bouchard, A. Gerbay, and K. Isaaz, "Robotic magnetic navigation for ablation of human arrhythmias," *Medical Devices (Auckland, NZ)*, vol. 9, p. 331, 2016.

[35] F. P. Melchels, J. Feijen, and D. W. Grijpma, "A review on stereolithography and its applications in biomedical engineering," *Biomaterials*, vol. 31, no. 24, pp. 6121–6130, 2010.

[36] P. Kanagaratnam, M. Koa-Wing, D. T. Wallace, A. S. Goldenberg, N. S. Peters, and D. W. Davies, "Experience of robotic catheter

ablation in humans using a novel remotely steerable catheter sheath," *Journal of Interventional Cardiac Electrophysiology*, vol. 21, no. 1, pp. 19–26, 2008.

[37] M. Koa-Wing, P. Kanagaratnam, D. Wallace, P. Lim, B. Willis, L. Alton, K. Aston, P. Sciberras, P. Kojodjojo, M. Wright *et al.*, "Initial experience of catheter ablation using a novel remotely steerable catheter sheath system," in *HEART*, vol. 93. BMJ PUBLISHING GROUP BRITISH MED ASSOC HOUSE, TAVISTOCK SQUARE, LONDON WC1H ..., 2007, pp. A60–A61.

[38] M. Schiemann, R. Killmann, M. Kleen, N. Abolmaali, J. Finney, and T. J. Vogl, "Vascular guide wire navigation with a magnetic guidance system: experimental results in a phantom," *Radiology*, vol. 232, no. 2, pp. 475–481, 2004.

[39] M. A. Tavallaei, Y. Thakur, S. Haider, and M. Drangova, "A magnetic-resonance-imaging-compatible remote catheter navigation system," *IEEE Transactions on Biomedical Engineering*, vol. 60, no. 4, pp. 899–905, 2012.

[40] Y. Yao, L. Ding, W. Chen, J. Guo, J. Bao, R. Shi, W. Huang, S. Zhang, and T. Wong, "The training and learning process of transseptal puncture using a modified technique," *Europace*, vol. 15, no. 12, pp. 1784–1790, 2013.